



## **Enhanced structural and spectroscopic properties of phosphosilicate nanostructures by doping with Al<sub>2</sub>O<sub>3</sub> ions and calcinations temperature**

**Mohamed M.ElOkr<sup>1</sup>, F.Metawe<sup>2</sup>, Amany M El-Nahrawy<sup>3</sup>,  
Basma A. A. Osman<sup>4</sup>**

<sup>1</sup>Physics Department, Faculty of Science, Al Azhar University, Nasr City, 11884 Cairo, Egypt.

<sup>2</sup>Department of Mathematical and Physical Engineering, Shoubra Faculty of Engineering Benha University, Egypt.

<sup>3</sup>Department of Solid State Physics, National Research Centre (NRC)-33 ElBohouth st., P.O.12622, Dokki, Giza, Egypt.

<sup>4</sup>Department of Basic Engineering Sciences, Benha Faculty Of Engineering, Benha University, Egypt.

**Abstract :** In the present work, Al<sub>2</sub>O<sub>3</sub> doped (80 P<sub>2</sub>O<sub>5</sub>: 20 SiO<sub>2</sub>) nanostructures were successfully prepared using a sol-gel process using triethylphosphate and tetraethylorthosilicate. We investigated the phase structure, microstructure and spectroscopic properties. Three different solutions were prepared by changing Al/P molar ratios such as 0, 10 and 15 in acidic condition. The obtained gel were aged at room temperature and dried at 100°C forming xerogel and subsequently calcined at different temperatures from 100 up to 700°C for 3h in air. The obtained oxides were characterized using X-ray diffraction (XRD), scanning electron microscopy (SEM) and Fourier transform infrared spectroscopy (FTIR). The micro-structural observations demonstrated that Al<sub>2</sub>O<sub>3</sub> content improved surface morphology of the nanostructure phosphosilicate. X-ray diffraction and FT-IR showed that the addition of Al<sub>2</sub>O<sub>3</sub> caused the formation of phosphosilicate network as P-O-Si, and formation of mixed phases based on P-O-Si-O-Al and P-O-Al separated from the phosphate matrix.

**Keywords:** Sol gel processes, phosphosilicate glass, aluminophosphosilicate nanoparticles, XRD, FTIR.

### **Introduction**

Recently, pure and doped phosphosilicate (PS) glasses have attracted considerable attention because of their capability to use in multi applications as optical, electronic, bioglasses due to bioactivity and biocompatibility<sup>1,2,3,4</sup>. At the same time, increasing interest has been devoted to sol gel phosphosilicate materials because of a chemical composition, ability to accommodate high concentrations of transition metal ions and chemical stability<sup>5,6</sup>. Sol gel phosphosilicate glass-ceramics are polycrystalline materials obtained by controlled crystallization of parent glasses<sup>6,7</sup>. In amorphous sol gel materials, to provide the glass network, we can use one or more glass former such as Si<sub>2</sub>O, P<sub>2</sub>O<sub>5</sub> or B<sub>2</sub>O<sub>3</sub> doped with some transition metals<sup>6</sup>. Depending upon the composition source of the parent glasses and the calcination temperature, various properties of the glass and glass-ceramic and dopents level can be precisely controlled<sup>7,8,9</sup>. These modified phosphosilicate glasses are

technologically and industrial important because of their excellent optical properties and chemical durability and are widely used in various applications<sup>7,10</sup>. Addition of network modifiers especially transition metals ions (M), where (M=Fe, Co, Al, Mn, Cu, Mo, W) to phosphosilicate network results in lowering the sintering temperature, more open structure, tetrahedral structural units. The metal ions were embedded during the preparation sol gel process at room temperature. The oxygen from the metal oxide as modifiers for the phosphosilicate glasses becomes part of the covalent network creating new structural units (P–O–Si, P–O–Al, Si–O–Al and P–O–Si–O–Al). The sol–gel process is attractive chemical method because it offers precise control of composition, high purity and homogeneity, easy processability, low cost and offers large-surface area systems<sup>11,12,13,14</sup>. Among the various compositions used through the sol–gel preparation, for phosphosilicate-based systems are triethylphosphate and tetraethoxysilane. Sol–gel method is an effective and simple technique to prepare inorganic, organic and organic/inorganic materials in different forms such as nano-wires nano-rods, monolithic, membranes, films and ceramics. The aim of this work, we have taken base phosphosilicate (PS) glass without and with nickel oxide as modifier prepared by sol gel process and calcined at different temperatures. The produced powders were characterized by X-ray diffraction (XRD), scanning electron microscopy (SEM) and Fourier transformed infrared (FTIR) spectroscopy. The relations between structural changes and the changes in physicochemical properties will be discussed as well. The objective of the present work was to investigate the effect of replacing varying contents (0, 10, 15 mol %) of P<sub>2</sub>O<sub>5</sub> with Al<sub>2</sub>O<sub>3</sub> in a phosphosilicate glass on the structural and spectroscopic properties.

## Experimental work

Pure phosphosilicate (80 P<sub>2</sub>O<sub>5</sub>: 20 SiO<sub>2</sub>) and doped with two different concentrations of Al<sub>2</sub>O<sub>3</sub> ions, ((80-x) P<sub>2</sub>O<sub>5</sub>: 20 SiO<sub>2</sub>: (x=0, 10&15) Al<sub>2</sub>O<sub>3</sub>) (based on mol%) nanoparticles were prepared by a sol–gel process. First, pure monolithic phosphosilicate were obtained by hydrolysis and condensation of triethylphosphate (TEP) (C<sub>2</sub>H<sub>5</sub>O)<sub>3</sub> P (O) as P<sub>2</sub>O<sub>5</sub>, tetraethoxysilane (C<sub>2</sub>H<sub>5</sub>O)<sub>4</sub> Si (TEOS, 99.999%, Sigma-Aldrich) as SiO<sub>2</sub> precursor in ethanol solution were hydrolyzed under vigorous stirring with distilled H<sub>2</sub>O containing HCl used as a catalyst. Then the Al<sup>3+</sup> ions were introduced in the process, by dissolving aluminum nitrate Al (NO<sub>3</sub>)<sub>3</sub>·9H<sub>2</sub>O in distilled H<sub>2</sub>O to the preceding precursors to get the desired concentration. These solutions were stirring for 2 h at room temperature. The resultant homogeneous solutions of monolith materials were filled in molds and aged one week in RT and then dried in a drying oven type GFL 71.5, at about 50°C for about 20 days until no shrinkage appears. Samples were clear and green color. Densification of gel was obtained, by calcination in air for 3h at temperature ranging from 100°C up to 700°C, in a muffle furnace with heating rate 5°C /min. X-ray diffraction (XRD) patterns of the prepared samples were recorded with an X-ray diffractometer using monochromatized CuK<sub>α1</sub> radiation of wavelength = 1.54056 Å. Crystallite sizes G were determined from the Scherer's equation ( $G = K\lambda / D \cos\theta$ ), where K is the Scherer constant (0.9),  $\lambda$ : is the wavelength, and D is the full width (in radians) of the peak at half maximum (FWHM) intensity. The value of G was confirmed by using the U-fit program. Fourier Transforms Infrared, were used to determine the individual frequencies and their intensities. The modern Fourier Transform infrared instruments are becoming more commonplace. The morphological feature was measured using scanning electron microscopy (SEM).

## Results and discussion

### 1. X-ray diffraction (XRD)

The X-ray diffraction patterns for pure phosphosilicate gel (80 P<sub>2</sub>O<sub>5</sub>: 20 SiO<sub>2</sub>) and doped with two different concentrations of aluminum ions in the formula ((80-x) P<sub>2</sub>O<sub>5</sub>: 20 SiO<sub>2</sub>: (x= 0, 10 &15) Al<sub>2</sub>O<sub>3</sub>) prepared by sol gel method are shown in Figs (1-4). The prepared samples are aged for one week at room temperature before drying at 80°C for 3 weeks and calcined at different temperature ranging from 100 up to 700°C for 3h in air. No peaks are observed for phosphate or phosphasilicate xerogel in the prepared samples calcined below 300°C except the characteristic broad hump at 2 $\theta$  between 16° and 27° attributed to amorphous silica gel, as shown in Fig. 1. It is suggested that xerogels prepared with the addition of different concentrations of Al<sub>2</sub>O<sub>3</sub> ions in phosphosilicate matrix was formed in short range ordering. This result attributed to the development of cross-linking of the P-O-, P-O-OH, Si-O- and -P-O-Si- bonds due to dehydration poly-condensation of the prepared systems and under the effect of Al<sub>2</sub>O<sub>3</sub> content in the phosphosilicate matrix. So that, weak peaks of phosphosilicate and aluminophosphosilicate begin to appear in the samples calcined at 300°C, these peaks are

ascribed to rhombohedra  $\text{Si}_5\text{P}_6\text{O}_{25}$  (JCPDS, no.70-2071), tetragonal  $\text{SiP}_2\text{O}_7$  (JCPDS, no.22-1320) phases corresponding to the formation of phosphosilicate system and hexagonal  $\text{Al}_{23}\text{Si}_5\text{P}_{20}\text{O}_{96}$  (JCPDS, no.52-1178), where these phases consists of isolated  $\text{SiO}_4$ ,  $\text{SiO}_6$  and  $\text{Si}_2\text{O}_7$  units linked by  $\text{PO}_4$  groups in the system phosphosilicate system to form  $\text{SiO}_2: \text{P}_2\text{O}_5$  nanostructures at lower temperature and linked with  $\text{AlO}_4$  to form  $\text{Al}_2\text{O}_3: \text{SiO}_2: \text{P}_2\text{O}_5$ <sup>15</sup>. By increasing the calcination temperature up to 500°C the three preceding phases appeared with higher intensities with different concentrations of  $\text{Al}_2\text{O}_3$  ions, as shown in Fig.3. This suggests that the presence of  $\text{Al}_2\text{O}_3$  ions in the sol-gel phosphosilicate helps form smaller phosphosilicate and aluminophosphosilicate matrices. Where, the removal of OH and organic groups, taking place at low temperature, makes the coordination of phosphosilicate matrix change greatly, due to the three dimensions polymerization (solid gel) and formation of glass network<sup>6,14</sup>. Fig.4 displays the XRD patterns for the prepared systems calcined at a higher temperature up to 700°C, an increase in the peaks intensities was observed due to the increase in crystalline structure and simultaneously the disappearance of the amorphous contribution. The prepared samples becomes more crystalline, with separation of the phases, where most of rhombohedra  $\text{Si}_5\text{P}_6\text{O}_{25}$  (JCPDS, no.70-2071) phase eliminated by increasing the calcinations temperature relative to tetragonal  $\text{SiP}_2\text{O}_7$  (JCPDS, no.22-1320) and hexagonal  $\text{Al}_{23}\text{Si}_5\text{P}_{20}\text{O}_{96}$  (JCPDS, no.52-1178). The crystallite sizes of the pure phosphosilicate and doped with two different concentrations of  $\text{Al}_2\text{O}_3$  ions were calculated from the FWHM (full width of half maximum) of the average of three majors diffraction peaks in the XRD patterns using Scherrer's formula<sup>16,17</sup>.

$$D = \frac{0.9\lambda}{B \cos \theta}$$

Where  $\lambda$  is the X-ray wavelength, the factor 0.9 assumes spherical particles and B is the full-width at half-maximum (FWHM) intensity of the diffraction line. The crystallite sizes of the pure phosphosilicate and doped with three different concentrations of  $\text{Al}_2\text{O}_3$  ions calcined at different temperatures from 200 up to 700°C, were found to be ranging from (7-38 nm).

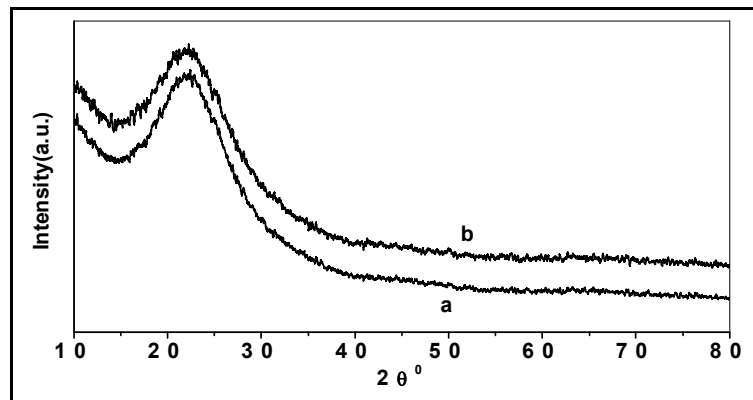


Fig. 1 XRD patterns of (a) pure phosphosilicate gel and (b) doped 15 mol % of  $\text{Al}_2\text{O}_3$  ions, calcined at 100°C.

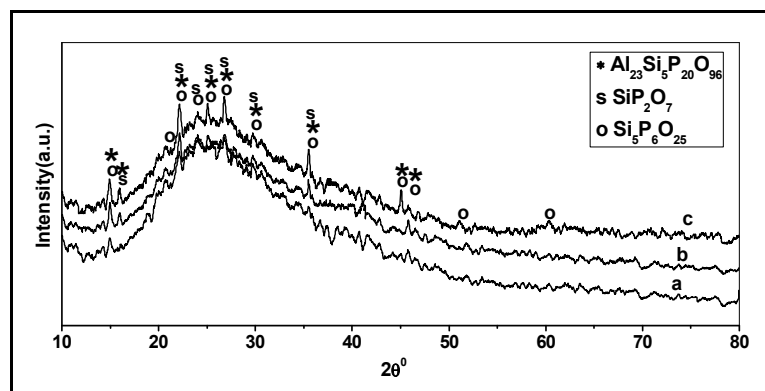


Fig.2 XRD patterns of (a) phosphosilicate gel and doped with two different concentrations of  $\text{Al}_2\text{O}_3$  ions (b) 10 and (c) 15 mol %, calcined at 300°C for 3h; \*  $\text{Al}_{23}\text{Si}_5\text{P}_{20}\text{O}_{96}$  phase, o  $\text{Si}_5\text{P}_6\text{O}_{25}$  phase and s  $\text{SiP}_2\text{O}_7$  phase.

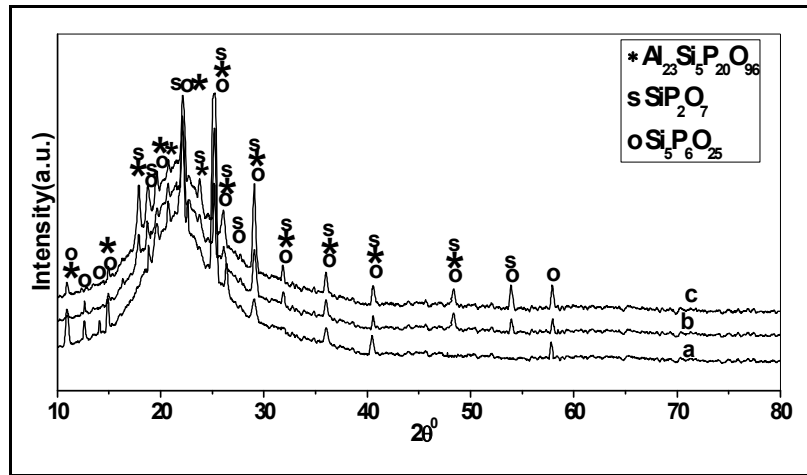


Fig.3 XRD patterns of (a) phosphosilicate gel and doped with two different concentrations of Al<sub>2</sub>O<sub>3</sub> ions (b) 10 and (c) 15 mol %, calcined at 500°C for 3h; \* Al<sub>23</sub>Si<sub>5</sub>P<sub>20</sub>O<sub>96</sub> phase, o Si<sub>5</sub>P<sub>6</sub>O<sub>25</sub> phase and s SiP<sub>2</sub>O<sub>7</sub> phase.

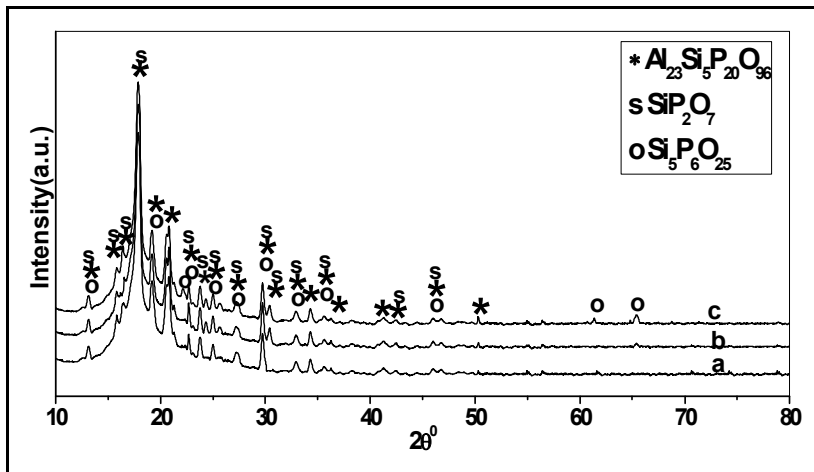
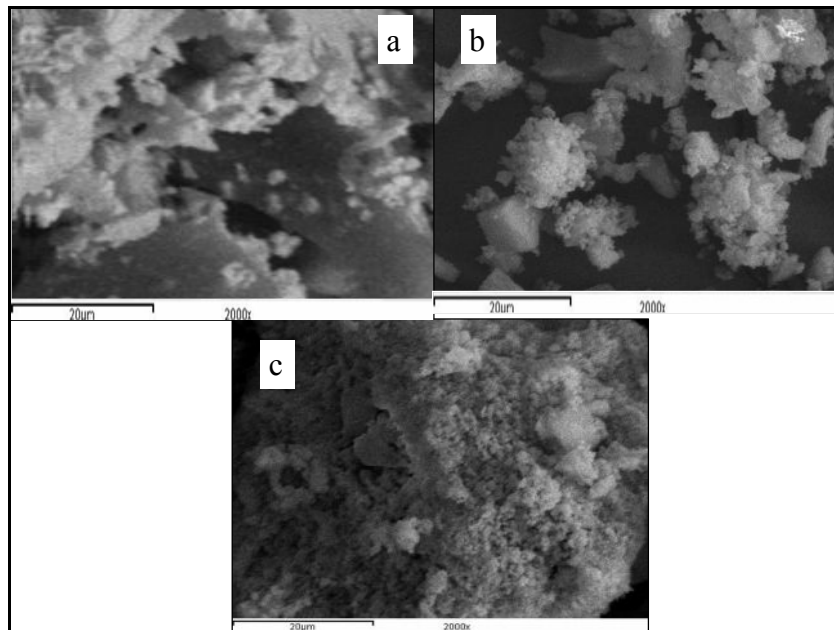


Fig.4 XRD patterns of (a) phosphosilicate gel and doped with two different concentrations of Al<sub>2</sub>O<sub>3</sub> ions (b) 10 and (c) 15 mol %, calcined at 700°C for 3h; \* Al<sub>23</sub>Si<sub>5</sub>P<sub>20</sub>O<sub>96</sub> phase, o Si<sub>5</sub>P<sub>6</sub>O<sub>25</sub> phase and s SiP<sub>2</sub>O<sub>7</sub> phase.

## 2. Scanning Electron Microscopy (SEM)

Figure 5 shows a SEM image of monolithic phosphosilicate (80 P<sub>2</sub>O<sub>5</sub>: 20 SiO<sub>2</sub>) phosphosilicate doped with (10 mol %) Al<sub>2</sub>O<sub>3</sub> ions, calcined at 300°C and magnifications of (2000x). As can be seen, some irregularly tiny and fine particles with large aggregates are observable in the micrograph confirms the nano-structure nature for the prepared samples with a high surface/volume ratio. The agglomerates exist in the prepared powders are attributed to the uncontrolled crystallinity during the transformation of the samples during calcinations at lower temperature.



**Fig. 5 SEM images of monolithic phosphosilicate calcined at (a) 300°C and (b) 700°C, and (c) phosphosilicate doped with 10 mol % of  $\text{Al}_2\text{O}_3$  ions, calcined 700°C for 3h in air.**

### 3. FTIR Spectra of pure phosphosilicate and doped with $\text{Al}_2\text{O}_3$ ions

Structural properties of nanostructure phosphor-silicate (80  $\text{P}_2\text{O}_5$ : 20  $\text{SiO}_2$ ) and doped with two different concentrations of  $\text{Al}_2\text{O}_3$  (10, 15, in mol %) were examined with FTIR spectroscopy. Fig. 6 shows the FTIR absorbance spectra the prepared samples calcined at 300°C, in a wide spectral region (400- 4000  $\text{cm}^{-1}$ ). The broad and sharp absorption at 3453  $\text{cm}^{-1}$  assigned to the stretching modes of OH groups, indicates that nonbridging oxygens are linked to hydrogens from phosphanol (P–OH), silanol moieties (Si–OH) and (Al–OH)<sup>14,18,19</sup>. The two weak absorption bands in the range from 3000  $\text{cm}^{-1}$  to 2900  $\text{cm}^{-1}$  are related to the –OH and organic groups<sup>6,20</sup>. These bands were observed in the glass systems containing  $\text{P}_2\text{O}_5$ , may be explained by the condensation of first P – OH and Si–OH in phosphosilicate and P – OH, Si–OH and Al– OH groups in aluminophospho-silicate (leading to P–O–P, Si–O–Si, P–O–Al, and Si–O–Al links) and the inorganic part becomes sufficiently rigid to form a real trap for the remaining OH groups, preventing their evacuation<sup>21</sup>. Where the hydrolysis mechanism during the sol gel process for triethylphosphate, tetraethylorthosilicate and aluminum nitrate as a sources for  $\text{P}_2\text{O}_5$ ,  $\text{SiO}_2$  and  $\text{Al}_2\text{O}_3$  through breakage of oxygen bridges results in changes in internal structure and depolymerization of system<sup>6,12,13</sup>. The absorption band at around 1635  $\text{cm}^{-1}$  is due to the deformation modes of  $\delta$  (H–O–H), attributed to bending vibration of crystalline water as interstitial molecules, which could come from KBr in the pellets and the adsorbed water<sup>22,23</sup>. The shoulder at 1221  $\text{cm}^{-1}$  may be attributed to P–O and/or P= O stretching vibration, because these bands occur in the fingerprint region(1320-1200  $\text{cm}^{-1}$ ), they cannot be used without some other indication that P is present, because C–O and O–H groups can also absorb strongly in these ranges. By increasing the  $\text{Al}_2\text{O}_3$  ions in phosphor-silicate the intense of the shoulder at 1221 decrease with increasing  $\text{Al}_2\text{O}_3$  content in the matrix this may be due to the formation of the stretching vibration of the Si–O–Si, Si–O–P and P–O–Al bonds<sup>24,25</sup>. The band located at 1091 $\text{cm}^{-1}$  is attributed to the vibration of Si–O–Al and P–O–Al bands for the nano-structure aluminophosphosilicate<sup>26,27</sup>. The characteristic vibration bands assigned to the P–O–P or/and P–O–Si bonds were not identified because they overlap with the characteristic band of the silica or phosphate matrix. Silica may exist inside the phosphorus clusters or at the interfaces between  $\text{P}_2\text{O}_5$  clusters and the  $\text{SiO}_2$  matrix in the form of P clusters or P–O–Si bonds, beside the Si–O–Al and P–O–Al bands distributed in the phosphosilicate matrix<sup>26,27</sup>. The vibration at 962  $\text{cm}^{-1}$  and 803  $\text{cm}^{-1}$  can be due to stretching vibrations of terminal P–O–, Si–O– and Si–O–P surrounded by P cation in pure phosphosilicate system or corresponding to Si–O–Al, P–O–Al and single or double bonds of P–O in the  $[\text{PO}_4]^{3-}$  group in aluminophosphosilicate matrix absorbed on the phosphosilicate surface, respectively<sup>28,29</sup>. The absorption band 466  $\text{cm}^{-1}$  is associated with Si–O–Si tetrahedral bending vibrations<sup>6,14</sup>. The phosphate-based glasses reveal major resonances at wave numbers of 557, 803, 962 and 1100  $\text{cm}^{-1}$ , which were associated with the P–O bonds in the phosphate network. The intense of the absorption bands at 1091, 962, 803, 557 and

466  $\text{cm}^{-1}$  indicating the formation of well-crystallized nano-sized pure phosphosilicate and doped with different concentrations of aluminum which were formed by the hydrolysis and condensation of phosphate, silica and aluminum precursors.

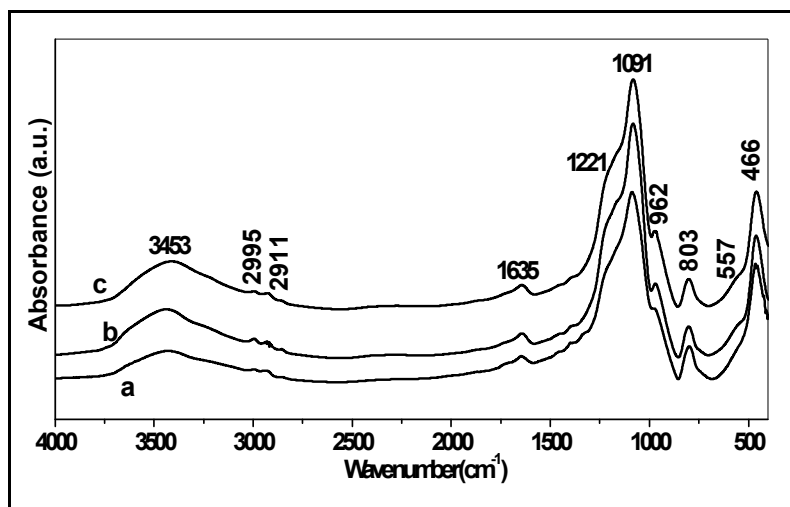


**Fig.6 FTIR absorbance spectra of monolithic phosphosilicate (a) and doped with two different concentrations of  $\text{Al}_2\text{O}_3$  ions (b) 10 and (c) 15 mol %, calcined at  $300^\circ\text{C}$  for 3h in air.**

## Conclusions

In the present paper, we have investigated the effect of two different concentrations of  $\text{Al}_2\text{O}_3$  ions on the structural and morphological properties of phosphosilicate matrix. These systems were prepared using sol-gel processes through the hydrolysis of the solutions of the P- and Si-alkoxides that reacted with HCL/water/ethanol at room temperature. The FTIR results indicate that nonbridging oxygens are linked to hydrogens from phosphanol (P–OH), silanol moieties (Si–OH) and (Al–OH). It was shown that the incorporation of  $\text{Al}_2\text{O}_3$  ions serve to polymerize the phosphosilicate glasses, resulting in both the increased chemical stability and the crystallinity.

## References

1. R. Murugavel, A. Choudhury, M.G. Walawalkar, R. Pothiraja, C.N.R. Rao, *Chem. Rev.* 108 (2008) 3549–3655.
2. Ar. G. Kannan, N. R. Choudhury, N. K. Dutta, *J of Electroanalytical Chemi.*, 641 (2010) 28–34..
3. R. Catteaux, I. G-Lebecq, F. Désanglois, F. Chai, J-C. Hornez, S. Hampshire, C. F-Houttemane, *Chemi. Engine. Research and Design*, 9 1 ( 2 0 1 3 ) 2420–2426.
4. V. Raj, M. S. Mumjitha, *Electrochimica Acta* 153 (2015) 1–11.
5. E. Metwalli, M. Karabulut , L. D.Sidebottom, M. M. Morsi, K. R. Brow, *J Non-Cryst Solids* 344(2004) 128–134.
6. A. M. Elnahrawy, A. Ibrahim, *New J. of Glass and Ceram.*, 4(2014) 42-47.
7. A. Ananthanarayanan , G.P.Kothiyal, L.Montagne, B.Revel, *J of Solid State Chem.*, 183 (2010) 1416–1422.
8. P.Riello, P. Canton, N. Comelato, S.Polizi, M. Verit, G. Fagherazzi, H. Hofmeister, S.Hopfe, *J.Non-Cryst.Solids*, 288(2001)127–139.
9. G. A. Khater, M. H. Idris, *Ceram.Int.*33(2007)233–238.
10. K. Zheng, S. Yang, J. Wang, C.Rüssel, C. Liu, W. Liang, *J of Non-Crystalline Solids* 358 (2012) 387–391
11. C.J. Brinker and G.W. Scherer, *Sol–Gel Science: The Physics and Chemistry of Sol–Gel Processing*, Academic Press, New York (1990).
12. A. M. El Nahrawy, Ali B. Abou Hammad, G. Turkey , M. M. M. Elnasharty, A. M. Youssef, *IJAETCS*, 2(2015) 9-14.
13. A. M Elnahrawy, *IJAETCS*, 2(2015) 15-18.

14. A. M. Elnahrawy, Y. S. Kim, A. I. Ali, *Jof Alloys and Compounds* 676 (2016) 432-439.
15. J. Perez-Pariente, F. Balas, J. Roman, A.J. Salinas, M. Vallet-Regí, *J. Biomed. Mater. Res.* 61 (2002) 524.
16. A.L. Patterson, The Scherrer formula for X-Ray particle size determination, *Phys.Rev*56(1939)978–982.
17. S.A. Hassanzadeh-Tabrizi, *Trans. Nonferrous Met. Soc. China* 21 (2011) 2443–2447.
18. H. Aguiar, E.L. Solla, J. Serra, P. González, B. León, N. Almeida, S. Cachinho, E.J.C. Davim, R.Correia, J.M. Oliveira, M.H.V. Fernandes, *J of Non-Crysta. Solids*, 354 (2008) 4075–4080.
19. X. Liu, X. Zhang, Z. Chen, X. Tan, *Ceram. Interna.*, 39 (2013) 5453–5458.
20. A. Charkhi, M. Kazemeini, S.J. Ahmadi, H. Kazemian, *Powder Techno.*, 231 (2012) 1–6.
21. G. Lakshminarayana, M. Nogami, I.V. Kityk, *J of Allo. & Comp.*, 509 (2011) 2238–2242.
22. D. L.Wood, *J. Am. Ceram. Soc.* 66(1982) 693-699.
23. Y-H. Han, A. Taylor, M. D. Mantle, K. M. Knowles, *J of Non- Cryst. Solids* 353 (2007) 313–320.
24. S. Sambandam, V. Ramani, *J. Power Sources* 170 (2007) 259–267.
25. K. Takeuchi, M. Terano, T. Taniike, *Polymer* 55 (2014) 1940-1947.
26. R. M. Filgueiras, G. LaTorre, L. L. Hench, *J Biomed Mater Res*, 27(1993)445–53.
27. S. Kongwudhiti , P. Prasertdam , W. Tanakulrungsank, M. Inoue, *J Mater Process Technol*, 136(2003)186-9.
28. I. Izquier-Barba, A.J.Salinas, M.Vallet-Regí, *Int.J.App. Glas.Sci.*4 (2)(2013) 149–161.
29. R.L. Siqueira, E.D.Zanotto, *J.Mater.Sci.:Mater.Med.*24(2013)365–379.

\*\*\*\*\*